Article
Vol. 22, No. 2, p. 241–252, April 2018
http://dx.doi.org/10.1007/s12303-017-0039-z
pISSN 1226-4806 eISSN 1598-7477
Geosciences Journal GJ

Prediction of natural fractures in the Lower Jurassic Ahe Formation of the Dibei Gasfield, Kuqa Depression, Tarim Basin, NW China

Wei Ju[1,2], Ke Wang[3], Guiting Hou[4]*, Weifeng Sun[2], and Xuan Yu[4]

[1]Key Laboratory of Coalbed Methane Resources and Reservoir Formation Process, Ministry of Education, China University of Mining and Technology, Xuzhou 221008, China
[2]School of Resources and Geosciences, China University of Mining and Technology, Xuzhou 221116, China
[3]PetroChina Hangzhou Research Institute of Geology, Hangzhou 310023, China
[4]School of Earth and Space Science, Peking University, Beijing 100871, China

ABSTRACT: The Lower Jurassic low porosity and low permeability Ahe Formation is the major reservoir of Dibei Gasfield in the Kuqa Depression, Tarim Basin. Natural fractures are important spaces for storage of hydrocarbons in low permeability reservoirs and can significantly improve the fluid flow capability; therefore, predicting the location and intensity of natural fractures in the Ahe Formation are of extreme importance. In the present study, the Late Himalayan paleotectonic stress field, the period of time when the majority of natural fractures generated in the Dibei Gasfield, was simulated and investigated with a three dimensional finite element (3D FE) model, which serves as a starting point for the prediction. Based on the principle of energy conservation and simulated paleotectonic stress field, the relationship between fracture density and stress parameter was established, and hence, natural fractures in the Ahe Formation of Dibei Gasfield were predicted. The results indicated that the development and distribution of natural fractures were primarily fault-controlled. Regions with well-developed natural fractures were mainly located in fault zones and around faults. Tectonic activities and ultra-high pressures were the dominant factors for natural fractures in the Ahe Formation. Regions with higher development degree of natural fractures in the Ahe Formation usually have a larger gas production; therefore, regions among Well Y1, B3, X1 and B2 should be focused in the Dibei Gasfield.

Key words: natural fracture, numerical simulation, low permeability reservoir, Dibei Gasfield, Ahe Formation

Manuscript received May 7, 2017; Manuscript accepted July 20, 2017

1. INTRODUCTION

The low permeability reservoir is an important type in sedimentary basins of China with the permeability generally less than 50×10^{-3} μm^2 (Li, 1997; Zeng and Li, 2009). Recently, several gasfields, including the Dibei Gasfield, have been discovered within the Cretaceous and Jurassic low porosity and low permeability reservoirs of Kuqa Depression, Tarim Basin, northwestern China (He et al., 2009; Lin et al., 2014). The Dibei Gasfield is located in the eastern Kuqa Depression (Fig. 1). The Lower Jurassic Ahe Formation, the major reservoir in the Dibei Gasfield, has an average porosity of 5.59% and average permeability of 0.76×10^{-3} μm^2 (Ju et al., 2013b, 2014c; Wei et al., 2015).

***Corresponding author:**
Guiting Hou
School of Earth and Space Science, Peking University, Beijing 100871, China
Tel: +86-10-62756422, Fax: +86-10-62751187, E-mail: gthou@pku.edu.cn

Natural fractures are the representation of crustal rocks that experienced multi-stages of tectonic activities and stress fields. In general, fractures, occurring at various scales in a hierarchical style, can strongly influence the performance of reservoirs around the world (e.g., Florez-Nino et al., 2005; Smart et al., 2009; Ju et al., 2014b, 2015; Ju and Sun, 2016). Natural fractures in low permeability reservoirs are important spaces for storage of hydrocarbons and can significantly improve the fluid flow capability (Aydin, 2000; Zeng and Li, 2009; Manzocchi et al., 2010; Ju et al., 2013b, 2014a). In addition, Zeng and Li (2009) indicated that the fracture permeability in low permeability sandstones was commonly larger than the matrix permeability by one or two orders of magnitude. Therefore, predicting the development and distribution of natural fractures in the low permeability Ahe reservoir is extremely important for both the exploration and exploitation in the Dibei Gasfield.

2. GEOLOGIC SETTINGS

The Tarim Basin, covering an area of about 5.6×10^5 km^2, is a typical superimposed petroliferous sedimentary basin in northwestern China (Jia et al., 1998). The Kuqa Depression, also known as the Kuche Depression, is located along the northern margin of the Tarim Basin between the South Tianshan Orogenic Belt and the Northern Tarim Uplift with an area of approximately 3.7×10^4 km^2 (Fig. 1; Chen et al., 2005; Zeng et al., 2010; Ju et al., 2014b). The depression is structurally NEE-SWW-trending with faults and related folds being the dominant structures (Fig. 1). Laterally, the Kuqa Depression can be divided into the northern monocline tectonic zone, Kelasu-Yiqikelike tectonic zone, Baicheng sag, Yangxia sag and Qiulitage tectonic zone from north to south (Fig. 1; Zeng et al., 2010).

The Kuqa Depression experienced a complex evolutionary history as a consequence of the northward Indian subcontinent and southward thrusting of the South Tianshan, and is recognized as one of the major depocenters along the margin of the Tarim Basin (Yin et al., 1998; Lu et al., 1999; Li et al., 2004; Zeng et al., 2010). The coal measure source rocks in the Kuqa Depression primarily developed during the Triassic to Jurassic (Fig. 2; Li et al., 2004; Zhao et al., 2005), rapidly subsided and began generating and expulsing hydrocarbons in the Neocene. A large number of gas reservoirs were formed in the depression during the end Pliocene to Pleistocene (Jia et al., 2003; Liu et al., 2008; Ju et al., 2014c).

The Dibei Gasfield is located in the central Yiqikelike tectonic zone of Kuqa Depression (Fig. 1). Based on seismic interpretations, faults, extensively developed in the Dibei Gasfield, were in a dominant orientation of NEE-SWW-trending with various sizes (Fig. 3).

In the Dibei Gasfield, the main gas source rocks were the Triassic Taliqike Formation and the Huangshanjie lacustrine hydrocarbon rocks, which were characterized by high organic abundance, III-type kerogen and high thermal evolution (Xing et al., 2012; Ju et al., 2014c; Lu et al., 2016). The Lower Jurassic

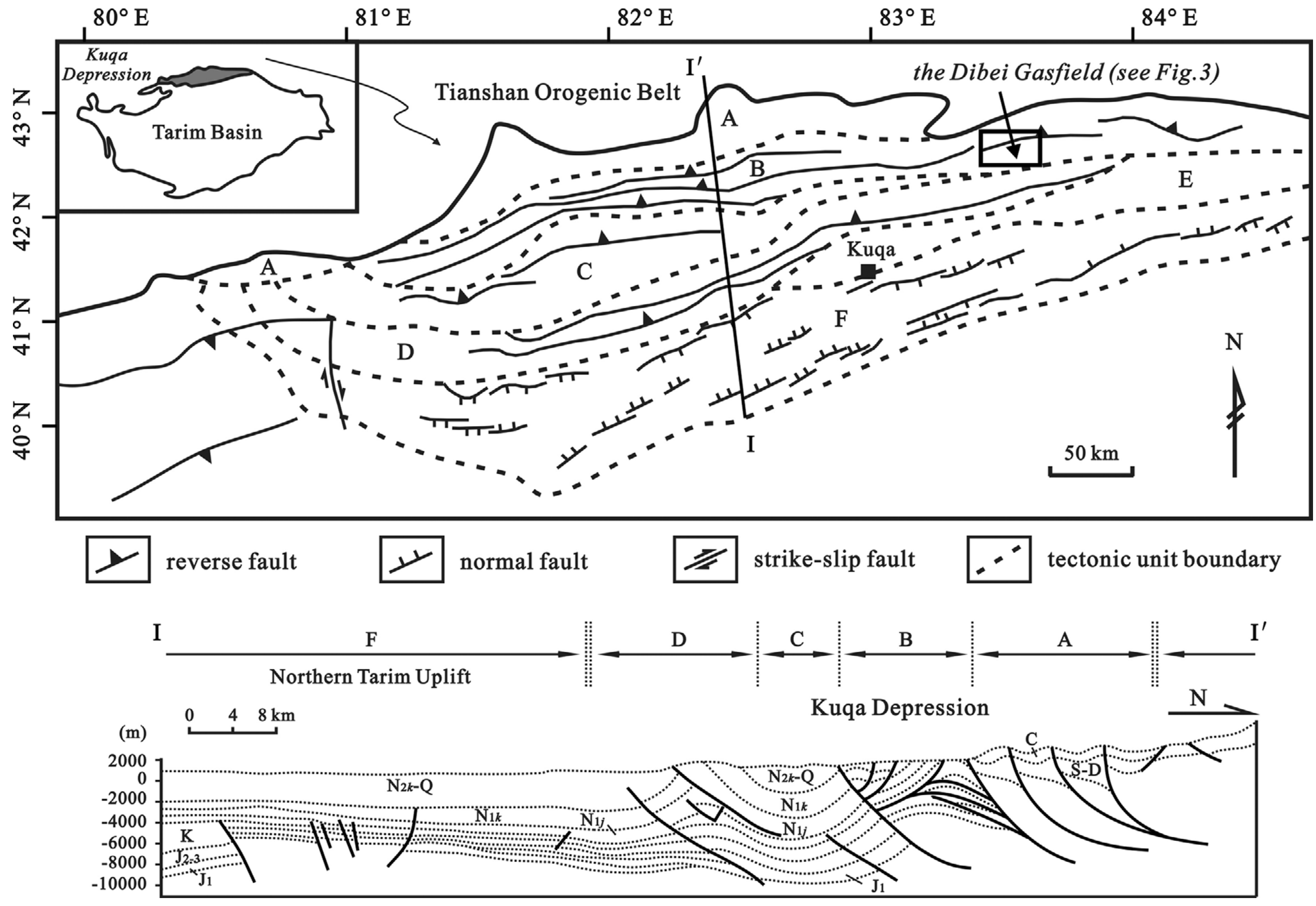

Fig. 1. Structure simplified map of the Kuqa Depression within the Tarim Basin, China (after Zeng et al., 2010). A-Northern monocline tectonic zone, B-Kelasu-Yiqikelike tectonic zone, C-Baicheng sag, D-Yangxia sag, E-Qiulitage tectonic zone, and F-Northern Tarim Uplift. S–D: Silurian to Devonian, C: Carboniferous, J_1: Lower Jurassic, J_{2+3}: Middle to Upper Jurassic, K: Cretaceous, N_{1j}: Jidike Formation, N_{1k}: Kangcun Formation, and N_{2k}–Q: Kuqa Formation to Quaternary.

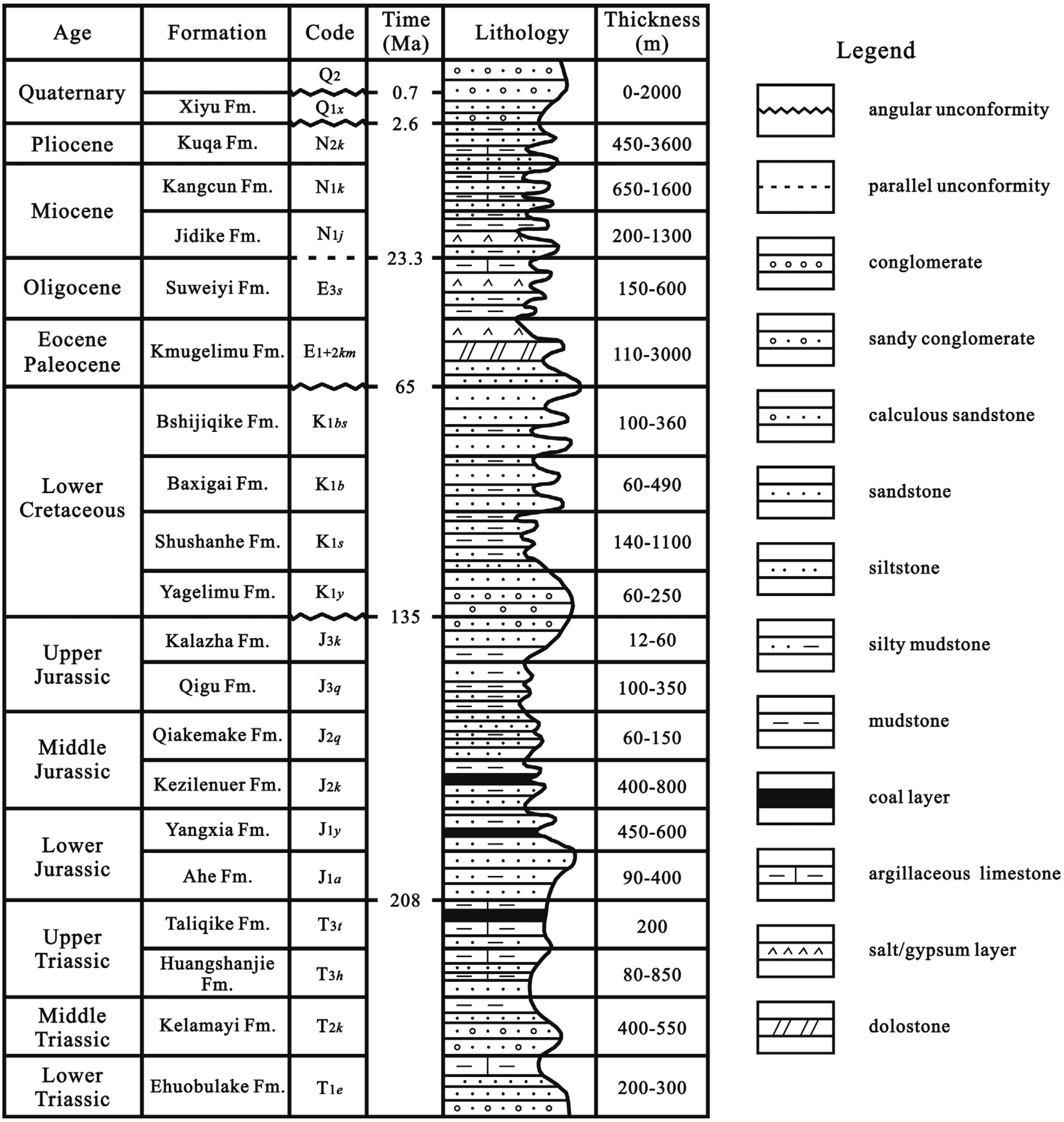

Fig. 2. Generalized stratigraphic column of the Kuqa Depression.

Ahe Formation was the primary reservoir in the Dibei Gasfield. The coal-bearing Jurassic Yangxia Formation and Kezilenuer Formation acted as good cap rocks (Fig. 2). These elements contributed to the favorable source-reservoir-cap rock combination in the Dibei Gasfield (Ju et al., 2014c; Lu et al., 2016).

The favorable rocks of the Lower Jurassic Ahe Formation in the Dibei Gasfield were sandy conglomerate, sandstone and siltstone (Figs. 2 and 4; Ju et al., 2013b). The Ahe Formation can further be divided into four members based on sedimentary characteristics (Fig. 4), namely, the J_1a_1, J_1a_2, J_1a_3 and J_1a_4. The J_1a_1 is a sandstone formation with mudstone interbedded. The rocks in the J_1a_2 and J_1a_4 are mainly sandy conglomerate, sandstone and siltstone. The J_1a_3 is a mudstone layer with a thickness of about 10 m (Fig. 4).

The Ahe Formation acted as the primary reservoir in the Dibei Gasfield; however, the development of natural fractures

http://dx.doi.org/10.1007/s12303-017-0039-z

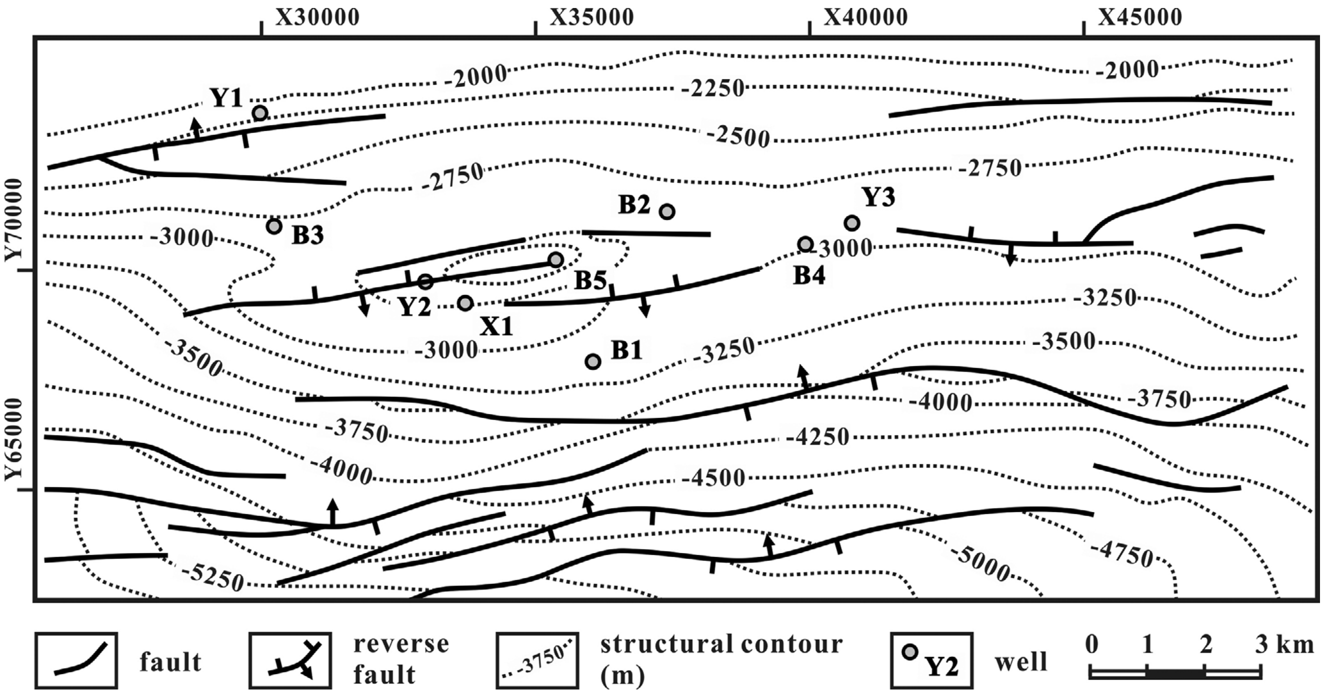

Fig. 3. Tectonic map of the top Lower Jurassic Ahe Formation in the Dibei Gasfield.

caused this formation has a strong heterogeneity (Fig. 5; Ju et al., 2013b; Lu et al., 2016). Furthermore, natural fractures can provide effective spaces for hydrocarbons and significantly improve the fluid flow capability; therefore, understanding the location and intensity of natural fractures in the Ahe Formation are extremely important in the Dibei Gasfield.

3. NUMERICAL SIMULATION OF STRESS FIELD

Tectonic stress is an important factor for generating fractures in rocks. The finite element (FE) technique is an effective approach to gain quantitative insights into the stress field in reservoirs (Fischer and Henk, 2013; Ju et al., 2013b, 2014a). In the present study, the FE method allowing complex geometries, lithological differences and fault morphology (e.g., Kattenhorn et al., 2000; Hou et al., 2010; Jiu et al., 2013; Ju et al., 2013b, 2014a; Ju and Sun, 2016) and the FE ANSYS software (version 12.0) were adopted to study the Late Himalayan paleotectonic stress field in the Dibei Gasfield of Kuqa Depression.

3.1. Geometry

In the present study, the initial 3D geometric model (Fig. 6) was constructed based on the structural conditions (Fig. 6) and sedimentary facies (Fig. 4) of the Lower Jurassic Ahe Formation. There is an assumption behind the model that the faults form first, and the fracture generation is then influenced by the effect of the faults on the stresses between the faults. The faults in the Dibei Gasfield were represented by weakness zones inside the model and they were further divided into different levels based on their sizes and scales (Fig. 6). The entire FE model was continuously meshed, and there were approximately 8228 nodes and 25265 elements within the FE model.

3.2. Material Properties

During FE modeling, the geological model was treated as an elastic body with units having different rock mechanical properties; therefore, material properties require to be assigned to the elements representing the Ahe Formation and faults. In the present study, the rock mechanics parameters of Ahe Formation (Table 1) were determined by mechanical experiments.

The definition of mechanical parameters in fault zones is extremely important to the results; however, exact values are unavailable. Based on previous studies (e.g., Jiu et al., 2013), in the present FE model, faults were defined as weakness zones with mechanical parameters (e.g., the Young's modulus) about 80% of the Ahe Formation. Poisson's ratios in fault zones were larger than those of the Ahe Formation, and their differences were typically between 0.02 and 0.10 (Table 1).

3.3. Boundary Conditions

Generally, the boundary conditions were difficult to be

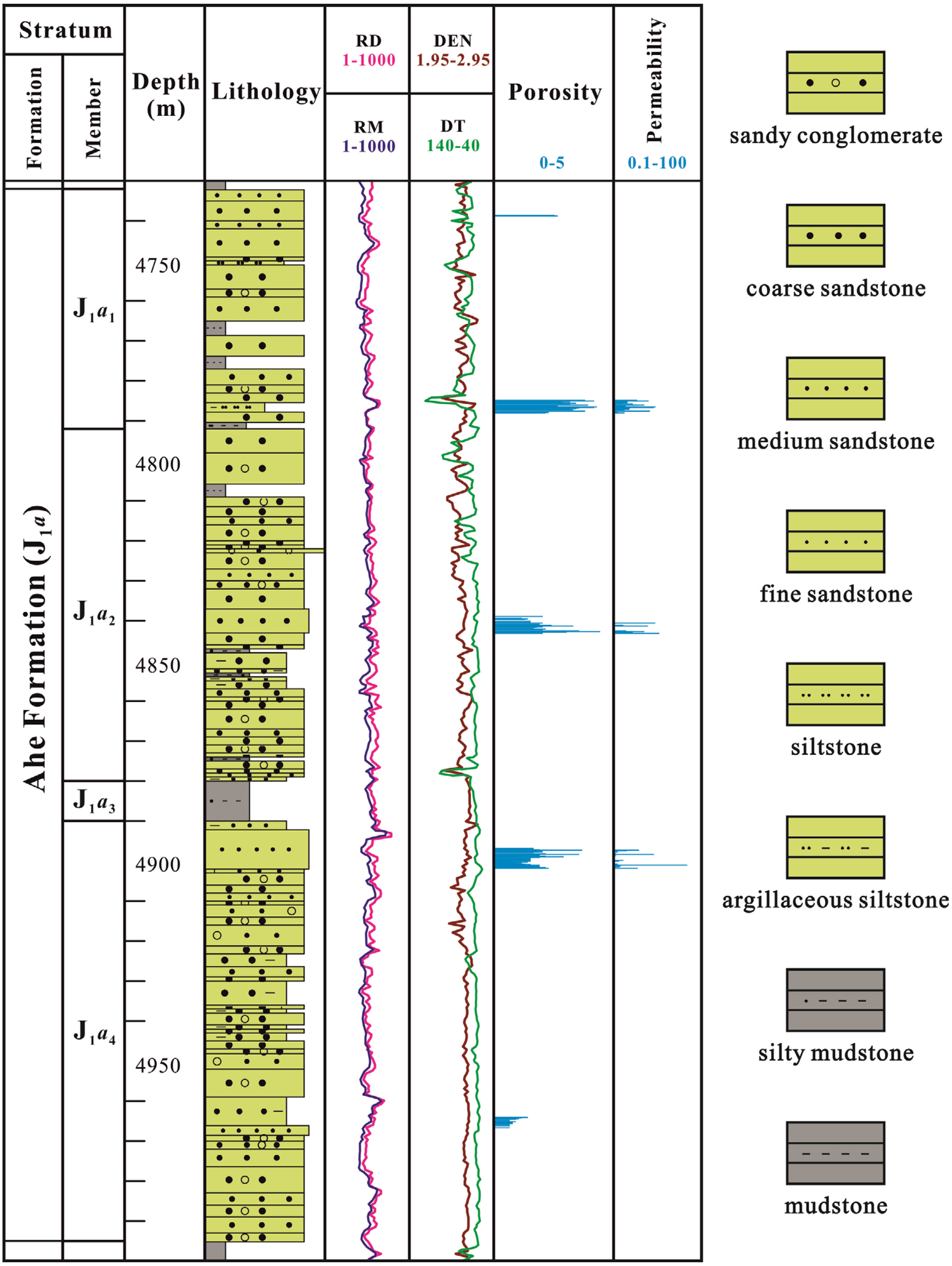

Fig. 4. Typical stratigraphic column of the Lower Jurassic Ahe Formation in the Dibei Gasfield. Symbols in the figure: RD: deep investigate double lateral resistivity log (Ω·m), RM: medium investigate double lateral resistivity log (Ω·m), DEN: density (g/cm^3), DT: acoustic (μs/m), porosity (%), and permeability (× 10^{-3} μm^2).

assumed because no clear geological boundaries can demarcate the study area from the rest parts of the Kuqa Depression. In the present analysis, the study area was nested within a larger rectangular parallelepiped (Fig. 6).

The vertical stress can usually be calculated from the bulk density of rocks based on Equation (1), and the horizontal stress

 http://dx.doi.org/10.1007/s12303-017-0039-z

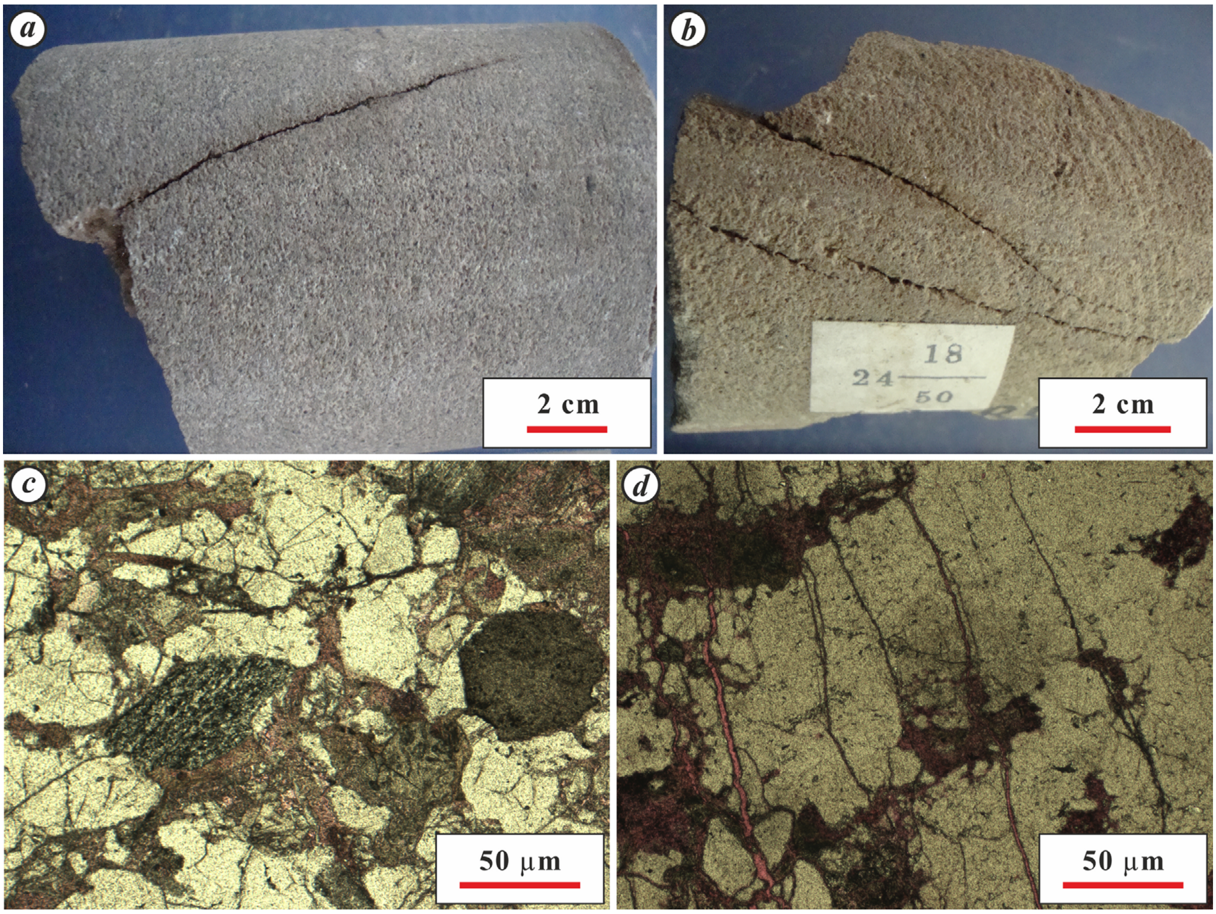

Fig. 5. Natural fractures in the Ahe Formation of the Dibei Gasfield. (a) Fractures in the cores of Well Y2, –4739.70 m; (b) Fractures in the cores of Well Y1, –4536.50 m; (c) Fractures in the thin section of Well Y2, –4785.05 m; (d) Fractures in the thin section of Well Y1, –4381.73 m.

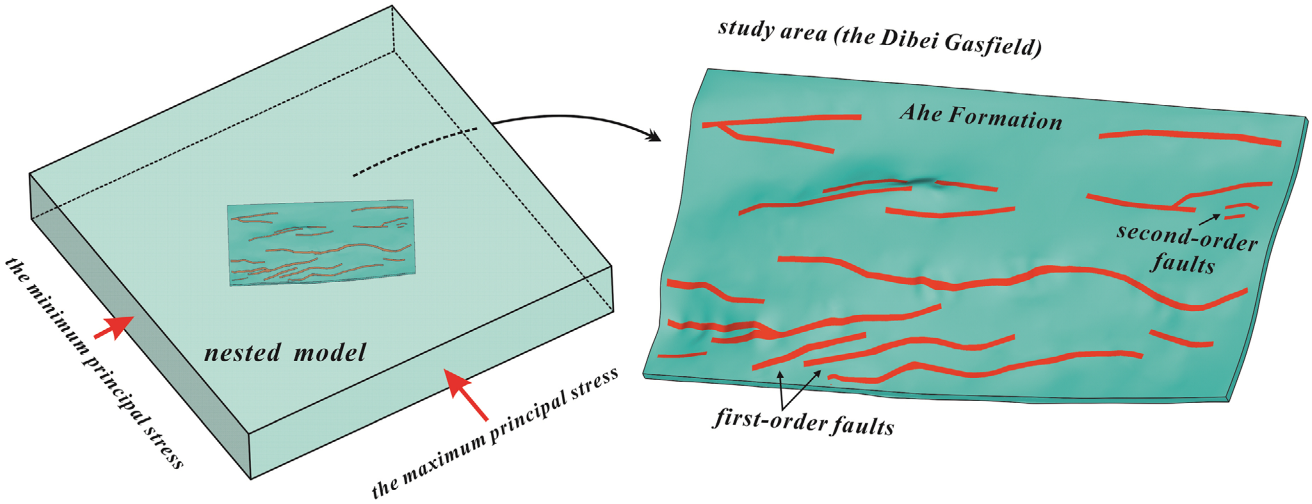

Fig. 6. The initial 3D geological model of the Ahe Formation in the Dibei Gasfield.

caused by the bulk density was less than 5 MPa in the Lower Jurassic Ahe Formation calculated by Equation (2) with a depth of about 1000 m.

$$\sigma_Z = \rho g h\,, \tag{1}$$

$$\sigma_{hs} = \sigma_Z \left(\frac{\upsilon}{1-\upsilon}\right)^{1/q}, \tag{2}$$

Table 1. Rock mechanics parameters in the Ahe Formation of the Dibei Gasfield

Layers	Density ρ (kg/m^3)	Young's modulus E (GPa)	Poisson's ratio υ	Internal friction angle θ(°)	Cohesion C (MPa)	Tensile strength σ_{TC} (MPa)
Ahe Formation	2510	12.51	0.23	44.77	21.38	2.51
Fault zones	2000	10.00	0.30	36.00	17.00	2.00
Nested model	2500	12.45	0.25	45.37	20.00	2.97

where σ_Z is the vertical stress, σ_{hs} is the horizontal stress caused by the bulk density, υ is the Poisson' ratio, ρ is the rock density, g is the gravitational acceleration, and q is a constant related to the non-linear compression, here q = 0.67 (Teeuw, 1971; Wang, 2001; Ju et al., 2015).

In the western Chinese Mainland, remote effects of the Cenozoic India-Eurasia collision and subsequent continuous compression caused the stress field and dominated the movements from the Himalayas to Tianshan Mountains (Tapponnier and Molnar, 1977). The Kuqa Depression experienced a ~N-S-trending compressional regime during the Late Himalayan period (Zhang et al., 2004, 2006; Zeng et al., 2010; Jiang et al., 2015). Based on regional analysis and previous studies (e.g., Zhang et al., 2006; Ju et al., 2013b), in the Dibei Gasfield, the maximum (σ_1) and minimum (σ_3) principal stress with a magnitude of $-(50 + \sigma_{hs})$ MPa and $-(10 + \sigma_{hs})$ MPa was applied in the NNW-SSE and NNE-SWW direction, respectively, during the FE modeling. The entire model was subjected to gravity loading in the vertical direction, which could be automatically applied in the ANSYS software. Besides, some appropriate displacement constraints were applied to the geological model to prevent it from rotation and rigid displacement, and to facilitate simulation (Jiu et al.,

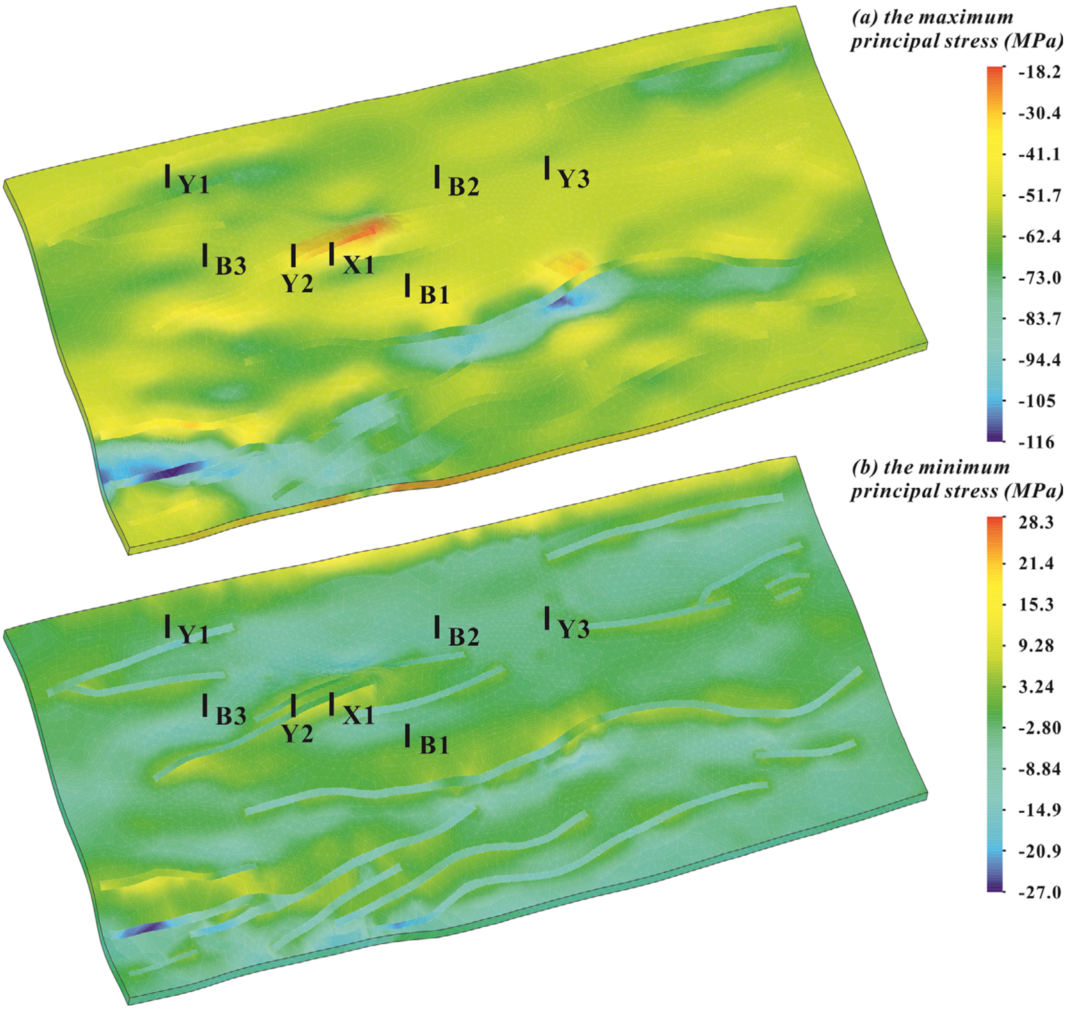

Fig. 7. The stress field in the Ahe Formation of the Dibei Gasfield, Kuqa Depression. (a) The maximum principal stress; (b) The minimum principal stress.

 http://dx.doi.org/10.1007/s12303-017-0039-z

2013; Ju et al., 2015). The top portion of the nested model was set as a free surface, whereas its bottom was fixed in the vertical direction. It is provided that compressive stresses were negative and tensile stresses were positive in this study.

3.4. Stress Field in The Dibei Gasfield

In the Ahe Formation of Dibei Gasfield, the σ_1 values varied between −116 MPa and −18.2 MPa (Fig. 7a), indicative of compression. The σ_3 values ranged from −27.0 MPa to 28.3 MPa (Fig. 7b), indicative of both compression and tension. The distributions of σ_1 and σ_3 indicated a fault-controlled pattern.

4. PREDICTION OF NATURAL FRACTURES

4.1. Method for Fracture Prediction

In petroleum geology, prediction of natural fractures in reservoirs was commonly based on the method of curvature analysis (McQuillan, 1973; Hennings et al., 2000) and/or seismic-based approaches (Muller et al., 1992; Gray et al., 2002), but far less with geomechanical modeling (Smart et al., 2009; Ju et al., 2013a, 2014b).

In this study, to show the patterns of natural fractures and stress field underground (Fig. 8), the Represent Element Volume (REV) is introduced, which is based on the following five assumptions (Ji et al., 2010; Feng et al., 2011): (i) natural fractures can cut through the REV, (ii) there are no fractures within the REV before applied forces, (iii) the REV is isotropic on the whole, (iv) the REV is a parallelepiped with the length of L_1, L_2 and L_3 in the direction of σ_1, σ_2 and σ_3, respectively, and (v) fractures in the σ_1–σ_3 plane are even spaced with the fracture planes parallel with σ_2.

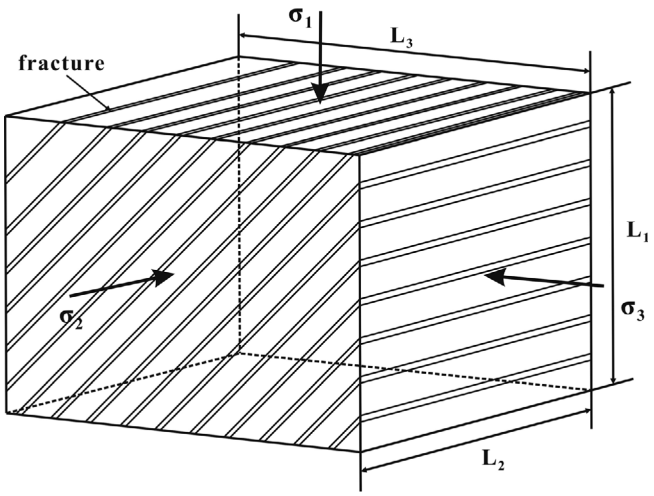

Fig. 8. The distribution of natural fractures in the REV (after Ji et al., 2010).

Based on geomechanical modeling above (Fig. 7) and the principle of energy conservation, the relationship between stress parameter and natural fracture density was confirmed (Eq. 3), and hence, the development and distribution of fractures were predicted on the basis of this relationship. According to previous studies (e.g., Ji et al., 2010; Feng et al., 2011; Wang et al., 2014), fracture density can be expressed as follows (Eqs. 3–6):

$$D_{vf} = \frac{\sigma_1\varepsilon_1 + \sigma_2\varepsilon_2 + \sigma_3\varepsilon_3}{2E(J_0 + \sigma_3 b)} - \frac{\sigma_d^2 - 2\nu\sigma_d(\sigma_2 + \sigma_3)}{4E(J_0 + \sigma_3 b)}, \quad (3)$$

$$\sigma_d = k\frac{2C\sin 2\alpha + (1 + \cos 2\alpha)\sigma_3}{1 - \cos 2\alpha}, \quad (4)$$

$$D_{lf} = \frac{2D_{vf}L_1L_3\sin\alpha\cos\alpha - L_1\sin\alpha - L_3\cos\alpha}{L_1^2\sin^2\alpha + L_3^2\cos^2\alpha}, \quad (5)$$

$$b = \frac{(1-P)(|\varepsilon| - |\varepsilon_0|)}{(1 + 9\sigma_n^*/\sigma_{nref})D_{lf}}, \quad (6)$$

where D_{vf} is the volumetric fracture density, D_{lf} is the linear fracture density, b is the fracture aperture, L_1 and L_3 are the lengths in Figure 8, E is the Young's modulus, ε_1, ε_2 and ε_3 are the maximum, medium and minimum principal strain, J_0 is the fracture surface energy with no confining pressures, σ_n* is the effective normal stress, ε_{nref} is the effective normal stress when the b decreases 10%, ε is the maximum tensile strain under the current stress state, ε_0 is the maximum tensile strain from experiments, α is the rupture angle, C is the cohesion, υ is the Poisson' ratio, P is the filling degree of fractures, here $P = 0.8$, and k is a coefficient, here $k = 0.85$.

4.2. Results and Analysis

In the Ahe Formation of Dibei Gasfield, the volumetric fracture density varied between 0 and 1.44 m^{-1} (Fig. 9). With the indicator of fracture density, well-developed natural fractures were mainly located in fault zones, fault tips and regions among faults, suggesting that the development and distribution of natural fractures in the Ahe Formation were primarily fault-controlled.

The error analysis was made to understand the modeling results based on the comparison between the predicted and measured fracture density in cores (Table 2). In generally, the error analysis is based on Equation (7) (Ju et al., 2013b).

$$r = \frac{|\text{predicted fracture density-measured fracture density}|}{\text{measured fracture density}}. \quad (7)$$

In the present study, fracture density in the Ahe Formation was measured in the Well Y1, Y2, Y3 and B3 in the Dibei Gasfield. The error analysis indicated that the predicted fracture density fitted the reality of the subsurface well (Table 2).

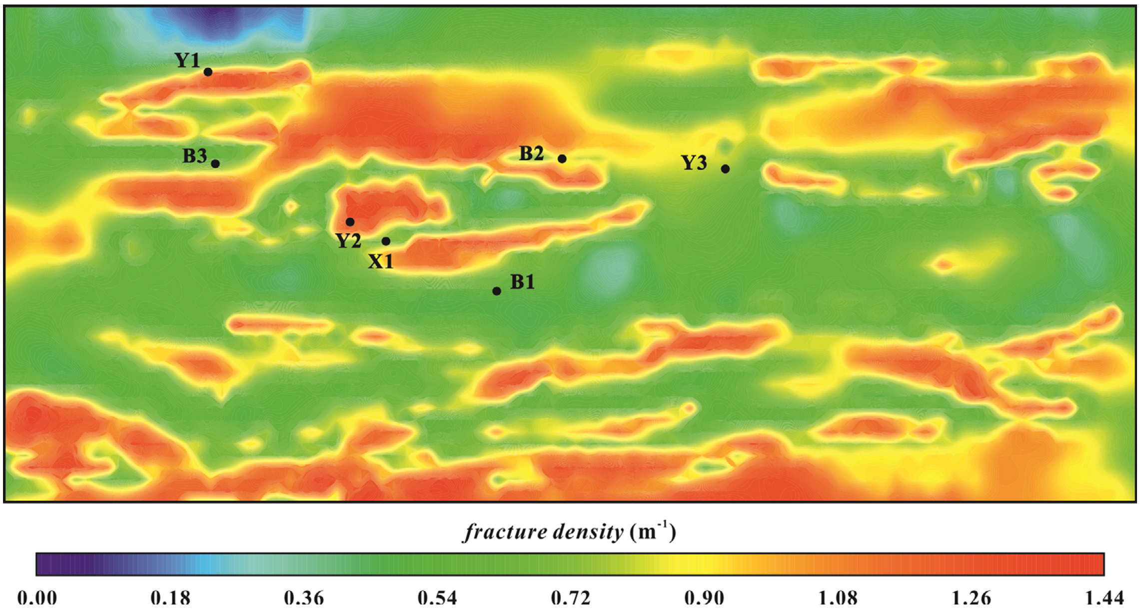

Fig. 9. Fracture density in the Ahe Formation of the Dibei Gasfield, Kuqa Depression.

Table 2. The error analysis in the Ahe Formation of the Dibei Gasfield

Wells	Predicted fracture density (m^{-1})	Measured fracture density in the core (m^{-1})	Error analysis
Y1	1.12	1.16	3.45%
Y2	1.36	2.19	37.90%
B3	0.62	0.56	10.71%
Y3	0.75	0.71	5.63%

However, it was abnormal in the Well Y2. The reason was that i) there were many small-scale faults in the Ahe Formation around the Well Y2, resulting in a higher rock failure degree; ii) furthermore, these highly ruptured rocks increased the difficulty in observing and measuring fractures in drill cores, which gave rise to the relatively abnormal high fracture density in the Well Y2 (Table 2).

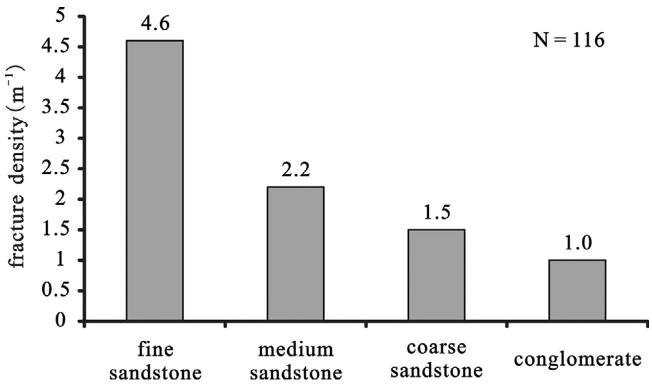

Fig. 10. Statistical graph showing the development of fractures in different lithologies of the Ahe Formation, Dibei Gasfield.

5. DISCUSSIONS

5.1. Factors for Natural Fractures

In general, several factors, categorized as non-tectonic factors (e.g., the lithology, mineral composition, mechanical property, thermal shrinkage, etc.) and tectonic factors (e.g., tectonic stress field, fault activities, etc.) (Ding et al., 2012; Ju and Sun, 2016), control the development and distribution of fractures in the Ahe Formation of Dibei Gasfield.

In the Ahe Formation of Dibei Gasfield, fault activities largely affected the development and distribution of fractures. Well-developed fractures were located in regions that are within fault zones and/or around faults (Fig. 9).

The lithology is an important non-tectonic factors in controlling the development of fractures (Hanks et al., 1997; Ding et al., 2012; Ju and Sun, 2016). The statistics of natural fractures in the Ahe Formation indicated that they were most developed in the fine sandstone (Fig. 10).

Fluid pressure might be a big issue for the development of tectonic fractures. High fluid pressures can promote the development of tectonic fractures by reducing the effective stress in formations (Cosgrove, 2001; Sibson, 2003; Ju and Sun, 2016). Generally, fluid pressure can be divided into four types: abnormal low pressure,

http://dx.doi.org/10.1007/s12303-017-0039-z

Table 3. The classification of pressure in reservoirs (after Du et al., 1995)

Types	Pressure coefficient	Pressure gradient (kPa/m)
abnormal low pressure	< 0.96	< 9.28
normal pressure	0.96–1.06	9.28–10.41
abnormal high pressure	1.06–1.38	10.41–13.58
ultra-high pressure	> 1.38	> 13.58

normal pressure, abnormal high pressure and ultra-high pressure based on the parameters of pressure coefficient and gradient (Du et al., 1995; Table 3). In the Dibei Gasfield, Yang and Zou (2004) and Liu et al. (2004) reported that the Lower Jurassic Ahe Formation experienced ultra-high pressures. The pressure coefficient in the Ahe Formation can reach as high as 1.7~1.8 based on the pressure tests from Well Y2 in the Dibei Gasfield (Yang and Zou, 2004).

5.2. Implications for Hydrocarbons

Generally, a lot of isolated pores were formed due to the dissolution of intergranular cement, rock fragments and mineral grain in reservoirs. Natural fractures can connect these isolated pores and provide larger spaces for gas accumulation (Aydin, 2000; Ju et al., 2014a). In addition, Jiang et al. (2015) indicated that natural fractures in low permeability reservoirs were able to improve the permeability for about 2~3 orders of magnitude (Fig. 11).

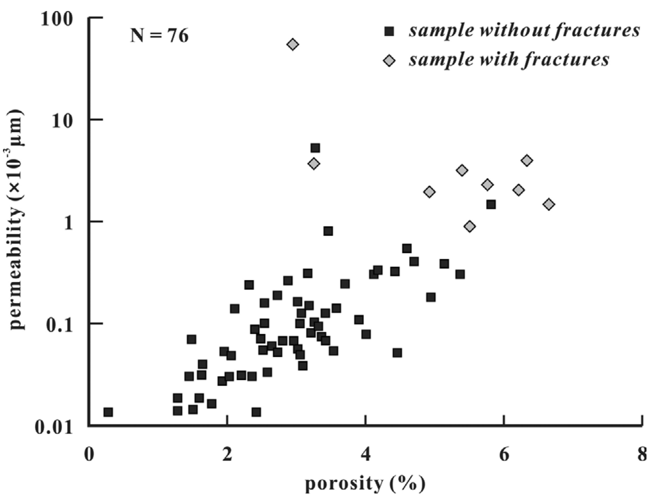

Fig. 11. Effects of fractures on the physical property of Ahe Formation in the Dibei Gasfield (after Jiang et al., 2015).

The development degree of natural fractures controlled gas production in the Dibei Gasfield. The average thickness of Ahe Formation was nearly the same in both wells of X1 and B3. Based on the interpretation of imaging logging, a total of 63 and 6 natural fractures were observed in the Ahe Formation of Well X1 and Well B3 (Table 4), respectively. The daily gas production in the Well X1 and Well B3 was 589861 m^3/d and 20768 m^3/d, respectively. Therefore, wells with larger fracture density usually resulted in higher gas production in the Dibei Gasfield (Table 4).

6. CONCLUSIONS

The Lower Jurassic Ahe Formation, the primary reservoir in the Dibei Gasfield, Kuqa Depression, is a typical reservoir with low porosity and low permeability. The development of natural fractures can provide effective spaces for hydrocarbons, significantly improve the fluid flow capability in the Ahe Formation.

In the present study, the Late Himalayan paleotectonic stress field, the period of time when the majority of natural fractures generated in the Dibei Gasfield, was simulated and investigated with a 3D FE model. The results indicated that the σ_1 and σ_3 values ranged from −116 MPa to −18.2 MPa, −27.0 MPa to 28.3 MPa, respectively. In order to predict the development and distribution of natural fractures in the low permeability Ahe Formation, the rock failure criteria were estimated and the relationship between in situ stress and parameters of natural fractures was confirmed based on the principle of energy conservation. The prediction of natural fractures showed that regions with well-developed fractures were primarily located in fault zones and around faults.

Among the factors for natural fractures, in the Dibei Gasfield, tectonic activities and ultra-high pressures control the development and distribution of fractures in the Ahe Formation. The development of fractures in the Ahe Formation could significantly improve the permeability and increase gas production; therefore, regions among Well Y1, B3, X1 and B2 may be focused in the Dibei Gasfield.

ACKNOWLEDGMENTS

We would like to express our gratitude to Prof. Yuxiang Lin and another anonymous reviewer for offering constructive

Table 4. The relationship between fracture density and gas production in the Dibei Gasfield (after Lu et al., 2016)

Wells	Thickness of the Ahe Formation (m)	Fractures interpreted from imaging logging (number/m)	Daily gas production (m^3/d)
X1	282	63	589861
B3	284	6	20768
B4	297	2	67320
B5	66	33	726416

suggestions and comments which improved this manuscript in many aspects. This work was supported by China Postdoctoral Science Foundation (2017T100419), National Science and Technology Major Project (2016ZX05044), Fundamental Research Funds for the Central Universities (2015XKZD07), and Priority Academic Program Development of Jiangsu Higher Education Institutions (PAPD).

REFERENCES

Aydin, A., 2000, Fractures, faults, and hydrocarbon entrapment, migration and flow. Marine and Petroleum Geology, 17, 797–814.

Chen, J., Lu, H.F., Wang, S.L., and Shang, Y.J., 2005, Geometric tests and their application to fault-related folds in Kuqa. Journal of Asian Earth Sciences, 25, 473–480.

Cosgrove, J.W., 2001, Hydraulic fracturing during the formation and deformation of a basin: A factor in the dewatering of low-permeability sediments. American Association of Petroleum Geologists Bulletin, 85, 737–748.

Ding, W.L., Li, C., Li, C.Y., Xu, C.C., Jiu, K., Zeng, W.T., and Wu, L.M., 2012, Fracture development in shale and its relationship to gas accumulation. Geoscience Frontiers, 3, 97–105.

Du, X., Zheng, H.Y., and Jiao, X.Q., 1995, Abnormal pressure and hydrocarbon accumulation. Earth Science Frontiers, 2, 137–148. (in Chinese with English abstract)

Feng, J.W., Dai, J.S., Ma, Z.R., Zhang, Y.J., and Wang, Z.K., 2011, The theoretical model between fracture parameters and stress field of low-permeability sandstones. Acta Petrolei Sinica, 32, 664–671. (in Chinese with English abstract)

Fischer, K. and Henk, A., 2013, A workflow for building and calibrating 3-D geomechanical models - a case study for a gas reservoir in the North German Basin. Solid Earth, 4, 347–355.

Florez-Nino, J.M., Aydin, A., Mavko, G., Antonellini, M., and Ayaviri, A., 2005, Fault and fracture systems in a fold and thrust belt: an example from Bolivia. American Association of Petroleum Geologists Bulletin, 89, 471–493.

Gray, D., Roberts, G., and Head, K., 2002, Recent advances in determination of fracture strike and crack density from P-wave seismic data. The Leading Edge, 21, 280–285.

Hanks, C.L., Lorenz, J., Teufel, L., and Krunhardt, A.P., 1997, Lithologic and structural controls on natural fracture distribution and behavior within the Lisburne Group, northeastern Brooks Range and north slope subsurface, Alaska. American Association of Petroleum Geologists Bulletin, 81, 1700–1720.

He, D.F., Zhou, X.Y., Yang, H.J., Lei, G., and Ma, Y.J., 2009, Geological structure and its controls on giant oil and gas fields in Kuqa Depression, Tarim Basin: a clue from new shot seismic data. Geotectonica et Metallogenia, 33, 19–32. (in Chinese with English abstract)

Hennings, P.H., Olson, J.E., and Thompson, L.B., 2000, Combining outcrop data and three-dimensional structural models to characterize fractured reservoirs: an example from Wyoming. American Association of Petroleum Geologists Bulletin, 84, 830–849.

Hou, G.T., Kusky, T.M., Wang, C.C., and Wang, Y.X., 2010, Mechanics of the giant radiating Mackenzie dyke swarm: a paleostress field modeling. Journal of Geophysical Research: Solid Earth, 115, 1–14.

Ji, Z.Z., Dai, J.S., and Wang, B.F., 2010, Quantitative relationship between crustal stress and parameters of tectonic fractures. Acta Petrolei Sinica, 31, 68–72. (in Chinese with English abstract)

Jia, C.Z., Wei, G.Q., Li, B.L., Xiao, A.C., and Ran, Q.G., 2003, Tectonic evolution of two-epoch foreland basins and its control for natural gas accumulation in China's mid-western areas. Acta Petrolei Sinica, 24, 13–17. (in Chinese with English abstract)

Jia, D., Lu, H.F., Cai, D.S., Wu, S.M., Shi, Y.S., and Chen, C.M., 1998, Structural features of northern Tarim Basin: implications for region tectonics and petroleum traps. American Association of Petroleum Geologists Bulletin, 82, 147–159.

Jiang, Z.X., Li, F., Yang, H.J., Li, Z., Liu, L.F., Chen, L., and Du, Z.M., 2015, Development characteristics of fractures in Jurassic tight reservoir in Dibei area of Kuqa Depression and its reservoir-controlling mode. Acta Petrolei Sinica, 36, 102–111. (in Chinese with English abstract)

Jiu, K., Ding, W.L., Huang, W.H., You, S.G., Zhang, Y.Q., and Zeng, W.T., 2013, Simulation of paleotectonic stress field within Paleogene shale reservoirs and prediction of favorable zones for fracture development within the Zhanhua Depression, Bohai Bay Basin, east China. Journal of Petroleum Science and Engineering, 110, 119–131.

Ju, W., Hou, G.T., Feng, S.B., Zhao, W.T., Zhang, J.Z., You, Y., Zhan, Y., and Yu, X., 2014a, Quantitative prediction of the Yanchang Formation Chang 6_3 reservoir tectonic fracture in the Qingcheng-Heshui area, Ordos Basin. Earth Science Frontiers, 21, 310–320. (in Chinese with English abstract)

Ju, W., Hou, G.T., and Hari, K.R., 2013a, Mechanics of mafic dyke swarms in the Deccan Large Igneous Province: palaeostress field modeling. Journal of Geodynamics, 66, 79–91.

Ju, W., Hou, G.T., Huang, S.Y., and Ren, K.X., 2013b, Structural fracture distribution and prediction of the Lower Jurassic Ahe Formation sandstone in the Yinan-Tuzi area, Kuqa Depression. Geotectonica et Metallogenia, 37, 592–602. (in Chinese with English abstract)

Ju, W., Hou, G.T., and Zhang, B., 2014b, Insights into the damage zones in fault-bend folds from geomechanical models and field data. Tectonophysics, 610, 182–194.

Ju, W. and Sun, W.F., 2016, Tectonic fractures in the Lower Cretaceous Xiagou Formation of Qingxi Oilfield, Jiuxi Basin, NW China. Part two: Numerical simulation of tectonic stress field and prediction of tectonic fractures. Journal of Petroleum Science and Engineering, 146, 626–636.

Ju, W., Sun, W.F., and Hou, G.T., 2015, Insights into the tectonic fractures in the Yanchang Formation interbedded sandstone-mudstone of the Ordos Basin based on core data and geomechanical models. Acta Geologica Sinica (English Edition), 89, 1986–1997.

Ju, Y., Sun, X.W., Liu, L.W., Xie, Y.N., and Wei, H.X., 2014c, Characteristics of Jurassic tight sandstone gas reservoir in Dibei area of Kuqa Depression, Tarim Basin. Xinjiang Petroleum Geology, 35, 264–267. (in Chinese with English abstract)

Kattenhorn, S.A., Aydin, A., and Pollard, D.D., 2000, Joints at high angles to normal fault strike: an explanation using 3-D numerical models of fault-perturbed stress fields. Journal of Structural Geol-

 http://dx.doi.org/10.1007/s12303-017-0039-z

ogy, 22, 1–23.
Li, D.P., 1997, The Development of the Low Permeability Sandstone Oil Field. Petroleum Industry Press, Beijing, 354 p. (in Chinese)
Li, Z., Song, W.J., Peng, S.T., Wang, D.X., and Zhang, Z.P., 2004, Mesozoic–Cenozoic tectonic relationships between the Kuqa subbasin and Tian Shan, northwest China: constraints from depositional records. Sedimentary Geology, 172, 223–249.
Lin, T., Yi, S.W., Ye, M.L., Ran, Q.G., Wei, H.X., and Liu, W.H., 2014, Characteristic of tight sandstone gas reservoir and the enrichment regularity in eastern Kuqa Depression. Geological Science and Technology Information, 33, 116–122. (in Chinese with English abstract)
Liu, G.D., Sun, M.L., Lv, Y.F., and Sun, Y.H., 2008, The effectiveness assessment of gas accumulation processes in Kuqa depression, Tarim Basin, Northwest China. Science in China Series D: Earth Sciences, 51, 117–125.
Liu, Y.K., Wu, G.H., Hu, J.F., Wang, J.N., Zheng, D.M., and Wu, J.G., 2004, Analyzing the characteristics of Yinan-2 gas reservoir in Kuche Depression of Talimu Basin. Natural Gas Industry, 24, 12–14. (in Chinese with English abstract)
Lu, H., Lu, X.S., Fan, J.J., Zhao, M.J., Wei, H.X., Zhang, B.S., and Lu, Y.H., 2016, Controlling effect of fractures on gas accumulation and production within the tight sandstone: a case study on the Jurassic Dibei gas reservoir in the eastern part of the Kuqa foreland basin, China. Journal of Natural Gas Geoscience, 1, 61–71.
Lu, H.F., Jia, D., Chen, C.M., Liu, Z.H., and Wang, G.Q., 1999, Nature and timing of the Kuqa Cenozoic structures. Earth Science Frontiers, 6, 215–221. (in Chinese with English abstract)
Manzocchi, T., Childs, C., and Walsh, J.J., 2010, Faults and fault properties in hydrocarbon flow models. Geofluids, 10, 94–113.
McQuillan, H., 1973, Small-scale fracture density in Asmari Formation of southwest Iran and its relation to bed thickness and structural setting. American Association of Petroleum Geologists Bulletin, 57, 2367–2385.
Mueller, M.C., 1992, Using shear waves to predict lateral variability in vertical fracture intensity. The Leading Edge, 11, 29–35.
Sibson, R.H., 2003, Brittle-failure controls on maximum sustainable overpressure in different tectonic regimes. American Association of Petroleum Geologists Bulletin, 87, 901–908.
Smart, K.J., Ferrill, D.A., and Morris, A.P., 2009, Impact of interlayer slip on fracture prediction from geomechanical models of fault-related folds. American Association of Petroleum Geologists Bulletin, 93, 1447–1458.
Tapponnier, P. and Molnar, P., 1977, Active faulting and tectonics in China. Journal of Geophysical Research, 82, 2905–2930.
Teeuw, D., 1971, Prediction of formation compaction from laboratory compressibility data (SPE paper 2973). Society of Petroleum Engineering Journal, 11, 263–271.
Wang, K., Dai, J.S., Zhang, H.G., Zhang, D.D., and Zhao, L.B., 2014, Numerical simulation of fractured reservoir stress sensitivity: a case study from Kuqa depression Keshen gas field. Acta Petrolei Sinica, 35, 123–133. (in Chinese with English abstract)
Wang, P., 2001, Tectonic Mechanic Principles of Oil-bearing Basins. Petroleum Industry Press, Beijing, 156 p. (in Chinese)
Wei, H.X., Xie, Y.N., Mo, T., Wang, Z.T., Li, L., and Shi, L.L., 2015, Fracture characteristic and its contribution to hydrocarbon accumulation in tight sandstone reservoir in Dibei gas pool in Kuqa Depression, Tarim Basin. Xinjiang Petroleum Geology, 36, 702–707. (in Chinese with English abstract)
Xing, H.S., Li, J., Sun, H.Y., Wang, H., Yang, Q., Shao, L.Y., Yang, D., and Yang, S., 2012, Differences of hydrocarbon reservoir forming between southwestern Tarim basin and Kuche mountain front. Natural Gas Geoscience, 23, 36–45. (in Chinese with English abstract)
Yang, S.G. and Zou, H.Y., 2004, A discussion on the genesis of Jurassic abnormal high pressure in the Yinan structural belt, Kuqa Depression. Henan Petroleum, 18, 20–24. (in Chinese)
Yin, A., Nie, S., Craig, P., Harrison, T.M., Ryerson, F.J., Qian, X.L., and Yang, G., 1998, Late Cenozoic tectonic evolution of the southern Chinese Tian Shan. Tectonics, 17, 1–27.
Zhang, M.L., Tan, C.X., Tang, L.J., Jiang, W., Yang, M.L., and Zeng, L.B., 2004, An analysis of the Mesozoic–Cenozoic tectonic stress field in Kuqa Depression, Tarim Basin. Acta Geoscientica Sinica, 25, 615–619. (in Chinese with English abstract)
Zhang, Z.P., Wang, Q.C., Wang, Y., and Li, T.J., 2006, Brittle structure sequence in the Kuqa Depression and its implications to the tectonic paleostress. Earth Science, 31, 309–316. (in Chinese with English abstract)
Zeng, L.B. and Li, X.Y., 2009, Fractures in sandstone reservoirs with ultra-low permeability: a case study of the Upper Triassic Yanchang Formation in the Ordos Basin, China. American Association of Petroleum Geologists Bulletin, 93, 461–477.
Zeng, L.B., Wang, H.J., Gong, L., and Liu, B.M., 2010, Impacts of the tectonic stress field on natural gas migration and accumulation: a case study of the Kuqa Depression in the Tarim Basin, China. Marine and Petroleum Geology, 27, 1616–1627.
Zhao, W.Z., Zhang, S.C., Wang, F.Y., Cramer, B., Chen, J.P., Sun, Y.G., Zhang, B.M., and Zhao, M.J., 2005, Gas systems in the Kuche Depression of the Tarim Basin: source rock distributions, generation kinetics and gas accumulation history. Organic Geochemistry, 36, 1583–1601.